small NANO MICRO

Lithography

Lithographically Fabricated Optical Antennas with Gaps Well Below 10 nm

*Wenqi Zhu, Mohamad G. Banaee, Dongxing Wang, Yizhuo Chu, and Kenneth B. Crozier**

Metal nanostructures that efficiently capture or radiate electromagnetic waves at optical frequencies offer a means to concentrate electromagnetic energy into deep subwavelength regions. Wessel noted that these structures can therefore be considered antennas.[1] Recent work has focused on more efficient designs, termed 'optical antennas', which employ small gaps or very sharp tips.[2–4] Optical antennas present opportunities for ultrasensitive spectroscopy, near-field scanning optical microscopy, and compact subwavelength light sources.[5–7] However, the achievable feature sizes are usually determined by fabrication, being approximately given by the gap size or tip sharpness. Here, we report a top-down fabrication procedure to fabricate pairs of nanoparticles separated by a controllable gap size that can be as small as 3 nm. As an application, we show that the enhancement factors of surface-enhanced Raman scattering (SERS) increase significantly for smaller gap sizes, indicating greatly enhanced electromagnetic fields within the gaps. We anticipate that the fabrication method we introduce here for nanoparticle pairs with nanoscale gaps would be useful not only for SERS, where it could potentially enable single-molecule sensitivity, but also for other applications in plasmonics.

Raman spectroscopy is a powerful analytical method, enabling molecules to be identified through their characteristic vibrational spectra. Through SERS, the Raman cross-section of molecules adsorbed to nanostructures can be increased by orders of magnitude. SERS has attracted renewed attention since the first demonstrations of single-molecule sensitivity.[8,9] Increasing the adoption of the SERS technique further, however, requires fabrication methods capable of routinely delivering reproducible substrates with high enhancement factors. Dimer structures, consisting of two metallic nanoparticles closely placed together, are the simplest optical antenna structures that are confirmed to be single-molecule SERS active.[10,11] It is believed that substantial electromagnetic fields generated in dimer gaps are one of the main enhancement mechanisms in single-molecule SERS.[12,13] This motivates the development of a reproducible method for the fabrication of dimers with very small gaps, especially below 10 nm. Dimers patterned by electron-beam lithography allow flexible design and controllable gap size, but face difficulties for gap sizes smaller than 10 nm, because of resolution limitations,[14] although such small features have been demonstrated using advanced lithography tools or special substrates.[15,16] There have also been numerous efforts in fabricating reproducible dimer structures with sub-10 nm gaps using chemical synthetic methods.[17,18] However, flexible control of dimer dimensions and location on device substrates is not easily available with chemical synthesis. Other proposed methods to achieve sub-10 nm gaps include break junctions,[19] electromigration,[20] electrodeposition,[21] and sacrificial layers.[22–25] The fabrication of resonant optical dimer antennas, however, was not demonstrated in these previous works. In this work, we demonstrate arrays of dimers with controllable gap size well below 10 nm by combining electron beam lithography with the use of sacrificial layers. The measured SERS enhancement factors increase almost by two orders of magnitude by reducing the gap size from ≈20 nm to ≈3 nm. This significant improvement confirms that there is a substantial electromagnetic field generated within dimer gaps.

The fabrication method is shown schematically in **Figure 1**a (see Supporting Information (SI) for details). The fabrication sequence was designed to yield a periodic array of paired gold nanoparticles (Figure 1b), in which each nanoparticle consisted of a rectangle 100 nm long, 80 nm wide, and 30 nm thick (Figure 1c). The outer edges of the nanoparticles were designed to be rounded, with a radius of curvature of 40 nm. As shown in Figure 1a, in Step (1), the left side of the dimer structure was defined by conventional electron beam lithography and lift-off processes. In the evaporation step, titanium (2 nm, adhesion layer), gold (30 nm), silver (30 nm) and chromium (10 nm) were deposited. In Step (2), the chromium layer was oxidized, either in ambient conditions (Figure 1d), or in oxygen plasma (Figure 1e) as discussed later in detail. As a result of the oxidation, the chromium layer expanded laterally on the order of several nanometers, resulting in it overhanging the edge of the silver layer. This can be seen by comparing Figure 1d,e with Figure 1f. In Step (3), the right side of the dimer was defined by a second electron beam lithography, in which alignment marks were employed. In the evaporation step, only titanium (adhesion layer) and gold were deposited. The length of the exposed pattern was chosen to be 144 nm, to result in an intentional overlap

W. Zhu, Dr. M. G. Banaee, D. Wang, Y. Chu, Prof. K. B. Crozier
School of Engineering and Applied Sciences
Harvard University
Cambridge, Massachusetts 02138, USA
E-mail: kcrozier@seas.harvard.edu

DOI: 10.1002/smll.201100371

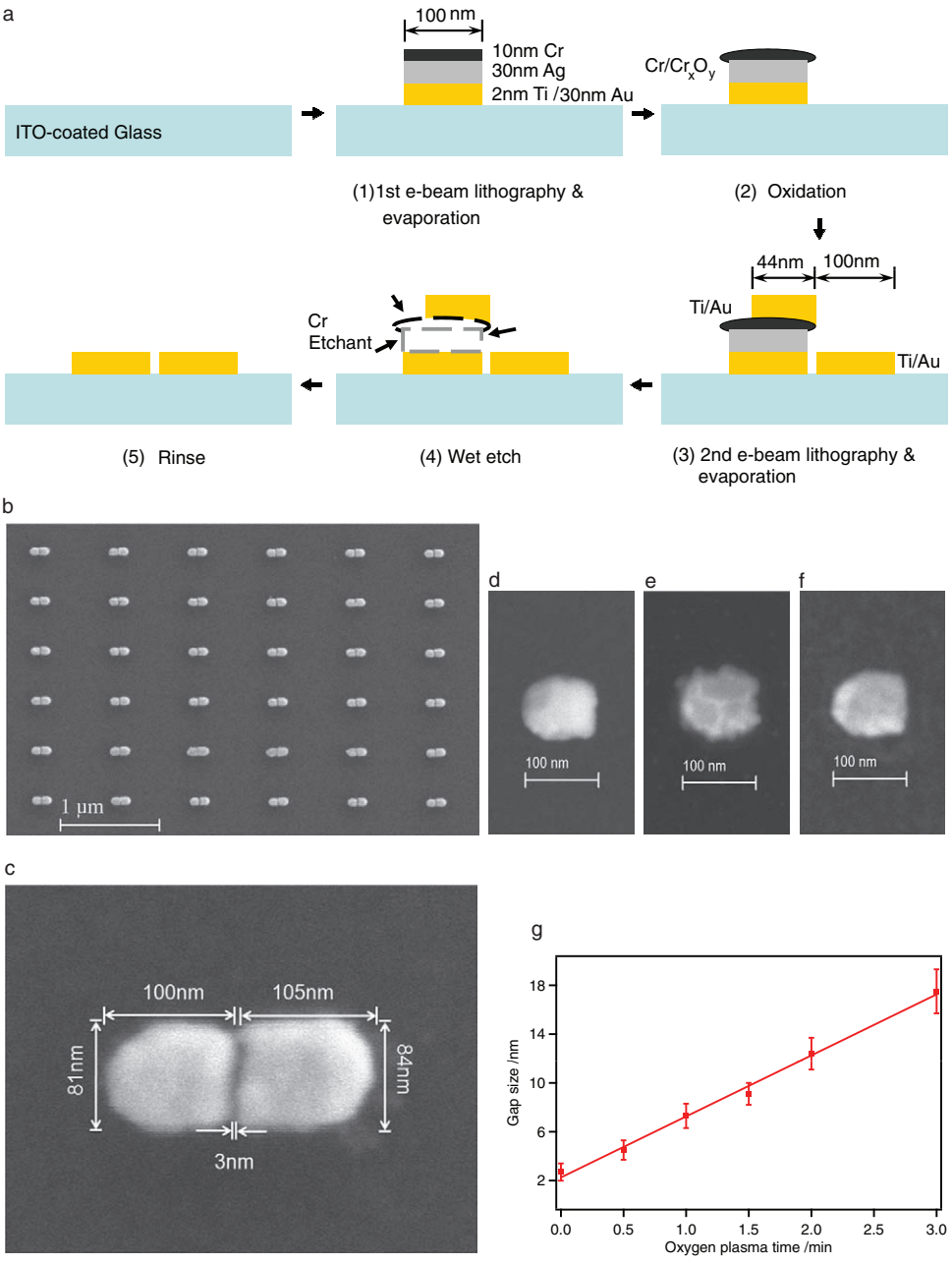

Figure 1. Device fabrication. a) Schematic diagram of fabrication process. b) SEM image of a fabricated dimer array obtained with 50k× magnification. c) SEM image of a dimer structure in the fabricated array of (b) obtained with 420k× magnification. d–f) SEM images of the left side of the dimer structure, after ambient oxidation (d), 2 min oxygen plasma (e), and pattern without silver/chromium layer for comparison, which is taken by etching the left-side pattern with chromium etchant just after the oxidation process (f). g) Gap size, determined from SEM, as a function of oxygen plasma time. Each error bar represents standard deviation of gap size for a particular dimer array, determined from nine randomly selected dimers within the array.

of 40 nm with the left side pattern, taking into account an anticipated lateral expansion of chromium layer of ≈4 nm. During evaporation, therefore, the length of the nanoparticle formed on the substrate is 100 nm, with the remainder (44 nm) being deposited onto the chromium layer. Through this method, the alignment error typically achieved (<10 nm) between the first and second lithography steps do not modify the gap size, and only results in an alteration of the length of the right side nanoparticle that is a small fraction of its total length. In Step (4), the silver and chromium layers were wet etched away, along with the gold layer on top of them deposited in the second evaporation process. Finally, the sample was rinsed thoroughly and dried in Step (5), resulting in an array of dimers. It can be seen that the chromium layer served as the mask layer in this fabrication: the thickness is selected to ensure that the final gap size is well below 10 nm. The silver served as the spacer layer: it formed an undercut structure beneath the chromium layer, in a similar manner to a bilayer resist in typical lift-off processes. It was found that the thickness of the silver layer is crucial to the overall yield

small NANO MICRO

of nanoscale gaps, as the chromium layer would be otherwise too thin to separate the gold patterns.

Figure 1b shows scanning-electron microscope (SEM) images of a fabricated dimer array. Of the 6 × 6 dimer structures in Figure 1b, 29 are considered 'good': a yield of ≈81%. Here, a 'good' dimer is defined as a structure with no connections within the gap and no broken patterns. We believe that gap connections may have come from titanium/gold residues during the wet etching in Step (4) in Figure 1a, or the evaporation in the Step (3) being not perfectly normal to the surface. Broken patterns, although not observed in Figure 1b, may come from the wet etching step when removing silver and chromium. Figure 1c shows a high magnification SEM of a fabricated dimer. From the SEM, the gap size, here defined as the separation between the closest two points within the gap, is found to be 3 nm (see SI). The standard deviation of the gap sizes measured from 9 dimers within this array is ≈1 nm. The fabrication results clearly demonstrate the ability of the method to fabricate dimer arrays with gaps well below 10 nm. We further demonstrate that the gap size can be effectively controlled by using oxygen plasma to carry out the oxidation of Step (2) in Figure 1a (see SI for details). Figure 1g shows the measured gap sizes produced with different plasma times. From the linear best fit to the data, the retrieved lateral oxidation rate is 5.0 nm min^{-1}, which is sufficiently slow to enable the fabrication of sub-10 nm gaps in a controllable manner. The gap size that results without the use of the oxygen plasma is ≈2 nm. However, it should be noted that in addition to Step (3) of Figure 1a, oxidation may occur in ambient conditions during other steps, such as resist baking for the second electron-beam lithographic step.

The optical properties of the fabricated dimer array were investigated by evaluating white light transmission spectra measured with polarized illumination (see SI). **Figure 2**a shows the extinction spectra of six typical samples retrieved from transmission spectra. Reducing the gap size red-shifts the resonance, which is consistent with theoretical predictions.[26] This is further confirmed by finite-difference time-domain (FDTD) simulation results (Figure 2b, see SI for details). Resonance peaks from simulation slightly differ from those from measurement; but the trend is consistent. It may be due to the fact that the simulations take the dielectric constant of gold to be that of bulk gold, but this may not be the case, since it varies with grain structure.[27] Simulated resonance linewidths (full-width half-maximum of extinction spectrum) are ≈50–70% smaller than measurements. This could be due to the nonuniformity of gap sizes within each array. It is also observed that the peak extinction cross-sections from measurement vary for different samples; this may be due to differences in fabrication yield between samples. For example, the yield of the 3 nm-gap sample is estimated to be ≈81%; while that of the 18 nm-gap structures is almost unity.

One of the major applications of optical antennas is for SERS. As discussed, it is generally accepted that higher enhancement can be achieved with smaller gaps.[13] However, few systematic studies on the variation in enhancement factor with gap size in the sub-10 nm range have been performed, owing to the difficulties associated with fabrication in this size regime. On the other hand, the fabrication

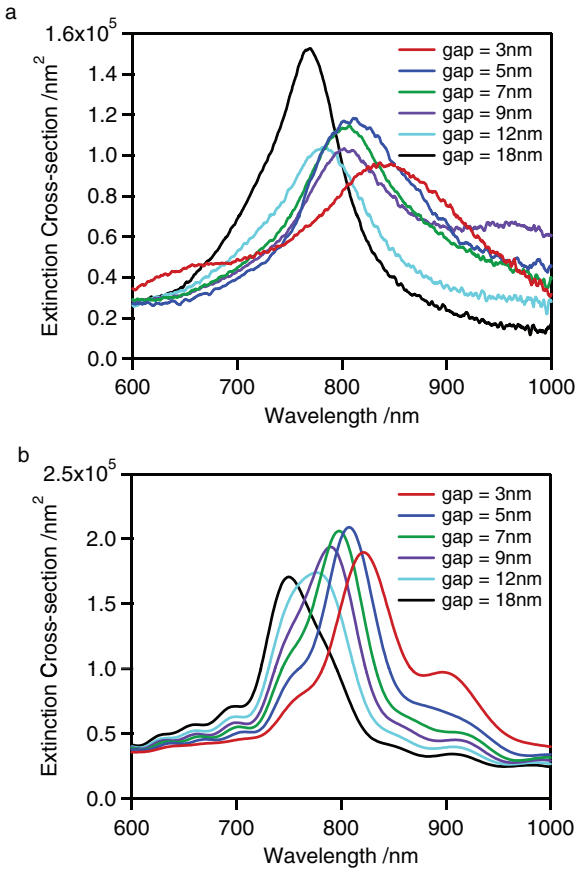

Figure 2. Retrieved extinction cross-sections for dimer arrays with different gap sizes, a) from measurement, b) from FDTD simulation.

method we introduce here enables such a study. We begin by comparing the SERS signals from samples with 3 and 12 nm gaps, as shown in **Figure 3**a,b. Self-assembled monolayers of benzenethiol were formed on both samples (see SI). The excitation wavelength for each sample was selected such that the mean value of laser wavelength and Stokes wavelength matched the peak resonance of the dimer array, to ensure the largest enhancement factor.[28] Even with the smaller laser power, the Raman counts from the 3 nm gap sample were much larger than those from the 12 nm gap sample. Indeed, the measured SERS enhancement factor (EF) for the 1072 cm^{-1} Raman line is 1.1×10^8 for the 3 nm-gap sample, and 4.4×10^6 for the 12 nm gap sample, representing a ≈25-fold improvement with the reduced gap size. Figure 3c,d show the mappings of retrieved EFs over 75 μm × 75 μm dimer arrays with gap sizes of ≈3 nm and ≈12 nm, respectively. To understand the mechanism of this enhancement better, the steady-state field distributions calculated by FDTD are shown in Figure 3e,f (see SI). The highest field intensity (square of electric field, $|E|^2$) enhancement in the 3 nm gap is ≈6 times larger than that in the 12 nm gap. A rough estimation of SERS EF is often based on $|E|^4$ approximation,[13,29] which indicates that the enhancement of the 3 nm gap antenna is ≈36 fold higher than the 12 nm gap antenna. This is generally consistent with the improvement from the SERS measurement, while a more rigorous estimation of electromagnetic EF (EM EF, see SI for details) is used later.

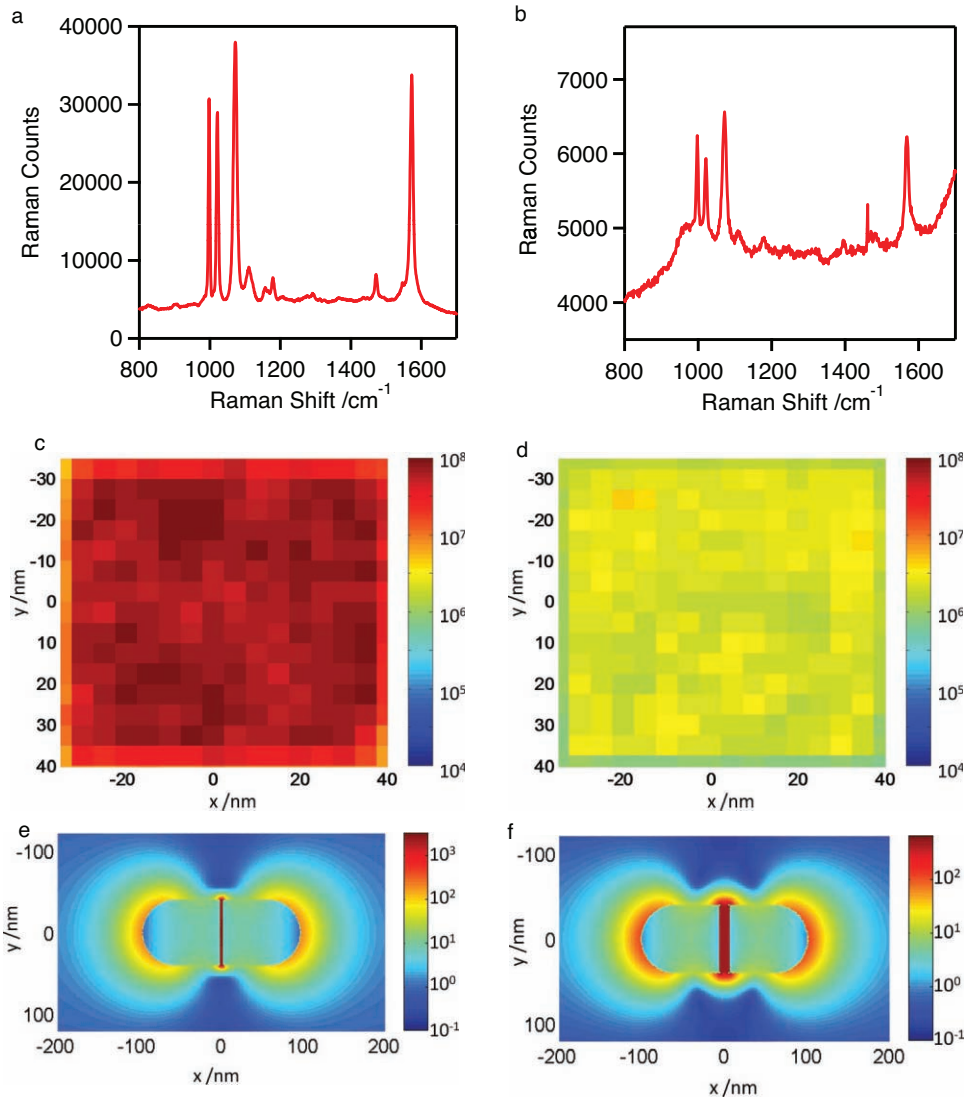

Figure 3. SERS measurement and simulation studies of device performance for dimer arrays with 3 nm and 12 nm gaps. a) Benzenethiol Raman spectrum measured on dimer array with 3 nm gaps. The excitation laser wavelength was 784 nm, and power at the sample was 0.82 mW. Raman signal integration time is 5 s. b) Benzenethiol Raman spectrum measured on dimer array with 12 nm gaps. The excitation laser wavelength was 750 nm, and power at the sample was 1.14 mW. Raman signal integration time is 5 s. c) Mapping of retrieved enhancement factors over 75 μm × 75 μm dimer array with gap sizes of ≈3 nm. d) Mapping of retrieved enhancement factors over 75 μm × 75 μm dimer array with gap sizes of ≈12 nm. e) Steady-state field intensity distribution ($|E|^2$) for dimer structure with 3 nm gaps calculated by FDTD. Plane-wave illumination was polarized along the antenna axes, at a wavelength of 821 nm. Field-intensity distribution is shown over center plane of dimer, 15 nm away from substrate. f) Log-scale steady-state field-intensity distribution for dimer structure with 12 nm gaps. Plane-wave illumination was polarized along the antenna axes, at a wavelength of 776 nm. Field intensity distribution is again shown over center plane of dimer, 15 nm away from substrate.

Identical measurements can be performed for dimer structures with other gap sizes. SERS EFs, as a function of dimer gap size, are mapped out in **Figure 4**. The laser excitation wavelengths were again selected for each dimer array to ensure maximum enhancement factor. Raman signal integration time for all the measurements were 5 s. In Figure 4, samples with the same gap size exhibit different enhancement factors. This is likely to be due to differences in structural morphology between samples with the same gap size. FDTD simulations were also performed for structures with various gap sizes to determine the expected EM EF. As shown in Figure 4, the simulated EM EFs were ≈75 times smaller than from the measured SERS EFs. Because the SERS measurements include the effects of chemical and electromagnetic enhancement,[10,30] we estimate that most of this discrepancy is due to chemical enhancement. Although detailed explanation requires close examination of individual dimer structure and is beyond the scope here, it is on the same order as that noted by Talley et al.,[31] although Lombardi and Birke find that in other cases it can be much higher.[32]

The SERS measurements reveal the effect of substantially enhanced electromagnetic field generated in dimer gaps.[33] From Figure 4, for gap size larger than 10 nm, the EFs are ≈10^6. This case means that the EF is not significantly improved over that obtained from isolated patterns,[14] representing weak enhancement within the gap between the two

NANO MICRO small

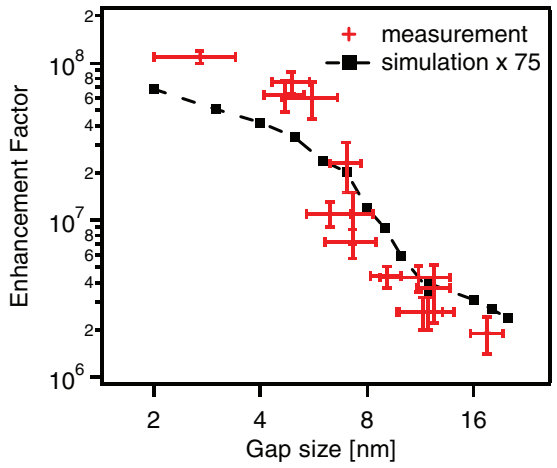

Figure 4. Measured SERS EF and simulated EM EF as a function of gap size. Each experimental data point was obtained from measurements made on a different sample. EF error bars represent the standard deviation in measured EF for each sample, determined from measurements made at nine points on the sample. Gap size error bars represent standard deviation of gap size for a particular dimer array, determined from nine randomly selected dimers within the array. EM EF was calculated by the FDTD method, and was multiplied by 75× to enable comparison to experimental data.

gold nanoparticles.[12] When the gap size is reduced to ≈10 nm or less, EF approaches ≈10^7. This is the strong enhancement case: due to the small distance between the particles, localized surface plasmon resonance of each particle is further amplified by the other, thereby significantly enhancing the field in the gap. When the gap size is further decreased to 5 nm or below, or even 3 nm as demonstrated here, EF can exceed 10^8, approaching the requirement for single-molecule detection.[34] It should be pointed out that typical SERS single-molecule SERS active dimer structure consist of two silver nanocrystals, which would provide a stronger surface plasmon resonance than the amorphous gold patterns employed here. Therefore the enhancement for these dimers is expected to be larger than that of the structures fabricated here. However, our lithographically fabricated dimer structure can be integrated with other plasmonic structures to achieve even higher enhancement factor,[35,36] and therefore represents progress toward the goal of reproducible single-molecule SERS substrates.

In conclusion, we have developed a fabrication procedure based on a sacrificial layer for the lithographic fabrication of optical antennas with gaps well below 10 nm. We demonstrate that the gap size can be effectively controlled by oxidizing the sacrificial layer using oxygen plasma. Localized electromagnetic fields can be significantly enhanced within the nanoscale gaps, as indicated by SERS measurements. This work enhances the ability to fabricate reproducible SERS substrates using a top-down method with a high enhancement factor. Moreover, by offering an accessible approach to fabricate features well below 10 nm, we anticipate that this technique will enable the fabrication of novel plasmonic structures otherwise not possible with standard techniques.

Experimental Section

Optical Measurements: Extinction cross-sections of dimer arrays were retrieved from white light transmission measurements. An objective lens (10×, NA = 0.25) was used to focus the incident polarized light onto the dimer array. The transmitted light was collected by another objective lens (50×, NA = 0.55) into a spectrometer equipped with a thermoelectrically-cooled charge-coupled device (CCD) array. An iris was used at the image plane of the objective to ensure that only the light transmitted through the array was detected.

SERS Measurements: Self-assembled monolayers of benzenethiol were formed on the gold nanostructures by immersing the samples in a solution of benzenethiol in ethanol (3 mM) for 2 h, rinsing with neat ethanol, and then blow drying with nitrogen. SERS measurements were carried out with a confocal Raman microscope (Renishaw inVia). The Raman signal was collected by an objective lens (20×, NA = 0.4) and input to a spectrometer containing a thermoelectrically-cooled CCD array.

Supporting Information

Supporting Information is available from the Wiley Online Library or from the author.

Acknowledgements

This work was supported by the Defense Advanced Research Project Agency (contract FA9550–08-1–0285). Fabrication was performed at the Harvard Center for Nanoscale Systems, which is supported by the National Science Foundation.

[1] J. Wessel, *J. Opt. Soc. Am. B* **1985**, *2*, 1538.
[2] R. D. Grober, R. J. Schoelkopf, D. E. Prober, *Appl. Phys. Lett.* **1997**, *70*, 1354.
[3] K. B. Crozier, A. Sundaramurthy, G. S. Kino, C. F. Quate, *J. Appl. Phys.* **2003**, *94*, 4632.
[4] L. Novotny, *Phys. Rev. Lett.* **2007**, *98*, 266802.
[5] P. Mühlschlegel, H.-J. Eisler, O. J. F. Martin, B. Hecht, D. W. Pohl, *Science* **2005**, *308*, 1607.
[6] H. Ko, S. Singamaneni, V. V. Tsukruk, *Small* **2008**, *4*, 1576.
[7] M. G. Banaee, K. B. Crozier, *ACS Nano* **2011**, *5*, 307.
[8] K. Kneipp, Y. Wang, H. Kneipp, L. T. Perelman, I. Itzkan, R. R. Dasari, M. S. Feld, *Phys. Rev. Lett.* **1997**, *78*, 1667.
[9] S. Nie, S. Emory, *Science* **1997**, *275*, 1102.
[10] A. M. Michaels, J. Jiang, L. E. Brus, *J. Phys. Chem. B* **2000**, *104*, 11965.
[11] H. Xu, E. J. Bjerneld, M. Käll, L. Börjesson, *Phys. Rev. Lett.* **1999**, *83*, 4357.
[12] J. Aizpurua, G. W. Bryant, L. J. Richter, F. J. Garcia de Abajo, B. K. Kelley, T. Mallouk, *Phys. Rev. B* **2005**, *71*, 235420.
[13] H. Xu, J. Aizpurua, M. Käll, P. Apell, *Phys. Rev. E* **2000**, *62*, 4318.
[14] N. Félidj, J. Aubard, G. Lévi, J. R. Krenn, M. Salerno, G. Schider, B. Lamprecht, A. Leitner, F. R. Aussenegg, *Phys. Rev. B* **2002**, *65*, 075419.
[15] A. W. Clark, J. M. Cooper, *Adv. Mater.* **2010**, *22*, 4025.
[16] M. D. Fischbein, M. Drndić, *Appl. Phys. Lett.* **2006**, *88*, 063116.

[17] H. Wang, C. S. Levin, N. J. Halas, *J. Am. Chem. Soc.* **2005**, *127*, 14992.
[18] D. K. Lim, K. S. Jeon, H. M. Kim, J. M. Nam, Y. D. Suh, *Nat. Mater.* **2010**, *9*, 60.
[19] J. Tian, B. Liu, X. Li, Z. Yang, B. Ren, S. Wu, N. Tao, Z. Tian, *J. Am. Chem. Soc.* **2006**, *128*, 14748.
[20] D. R. Ward, N. K. Grady, C. S. Levin, N. J. Halas, Y. Wu, P. Nordlander, D. Natelson, *Nano Lett.* **2007**, *7*, 1396.
[21] L. Qin, J. Jang, L. Huang, C. A. Mirkin, *Small* **2006**, *3*, 86.
[22] J. Tang, Y. Wang, C. Nuckolls, S. J. Wind, *J. Vac. Sci. Technol. B* **2006**, *24*, 3227.
[23] A. Fursina, S. Lee, R. G. S. Sofin, I. V. Shvets, D. Natelson, *Appl. Phys. Lett.* **2008**, *92*, 113102.
[24] H. Im, K. C. Bantz, N. C. Lindquist, C. L. Haynes, S. Oh, *Nano Lett.* **2010**, *10*, 2231.
[25] S. Lee, J. Shin, Y. Lee, S. Fan, J. Park, *Nano Lett.* **2010**, *10*, 296.
[26] E. Prodan, C. Radloff, N. J. Halas, P. Norlander, *Science* **2003**, *302*, 419.
[27] K. Chen, V. P. Drachev, J. D. Borneman, A. V. Kildishev, V. M. Shalaev, *Nano Lett.* **2010**, *10*, 916.
[28] A. D. McFarland, M. A. Young, J. A. Dieringer, R. P. Van Duyne, *J. Phys. Chem. B.* **2005**, *109*, 11279.
[29] E. C. Le Ru, P. G. Etchegoin, *Chem. Phys. Lett.* **2006**, *423*, 63.
[30] S. Saikin, R. Olivares-Amaya, D. Rappoport, M. Stopa, A. Aspuru-Guzik, *Phys. Chem. Chem. Phys.* **2009**, *11*, 9401.
[31] C. E. Talley, J. B. Jackson, C. Oubre, N. K. Grady, C. W. Hollars, S. M. Lane, T. R. Huser, P. Nordlander, N. J. Halas, *Nano Lett.* **2005**, *5*, 1569.
[32] J. R. Lombardi, R. L. Birke, *J. Phys. Chem. C* **2008**, *112*, 5605.
[33] S. Lal, N. K. Grady, G. P. Goodrich, N. J. Halas, *Nano Lett.* **2006**, *6*, 2338.
[34] E. C. Le Ru, E. Blackie, M. Meyer, P. G. Etchegoin, *J. Phys. Chem. C* **2007**, *111*, 13794.
[35] Y. Chu, M. G. Banaee, K. B. Crozier, *ACS Nano* **2010**, *4*, 2804.
[36] D. Wang, T. Yang, K. B. Crozier, *Opt. Express* **2011**, *19*, 2148.

Received: February 22, 2011
Revised: March 17, 2011
Published online: